

# FZD10-targeted $\alpha$ -radioimmunotherapy with $^{225}\text{Ac}$ -labeled OTSA101 achieves complete remission in a synovial sarcoma model

Hitomi Sudo<sup>1</sup> | Atsushi B. Tsuji<sup>1</sup>  | Aya Sugyo<sup>1</sup> | Yosuke Harada<sup>2</sup> | Satoshi Nagayama<sup>3</sup> | Toyomasa Katagiri<sup>4</sup>  | Yusuke Nakamura<sup>5</sup> | Tatsuya Higashi<sup>1</sup>

<sup>1</sup>Department of Molecular Imaging and Theranostics, National Institutes for Quantum and Radiological Science and Technology (QST), Chiba, Japan

<sup>2</sup>OncoTherapy Science Inc., Kanagawa, Japan

<sup>3</sup>Department of Surgery, Uji Tokushukai Medical Center, Kyoto, Japan

<sup>4</sup>Division of Genome Medicine, Institute of Advanced Medical Sciences, Tokushima University, Tokushima, Japan

<sup>5</sup>Cancer Precision Medicine Center, Japanese Foundation for Cancer Research, Tokyo, Japan

## Correspondence

Atsushi B. Tsuji and Tatsuya Higashi, Department of Molecular Imaging and Theranostics, National Institutes for Quantum and Radiological Science and Technology, 4-9-1 Anagawa, Inage, Chiba 263-8555, Japan.  
Emails: tsuji.atsushi@qst.go.jp (ABT) and higashi.tatsuya@qst.go.jp (TH)

## Funding information

Japan Society for the Promotion of Science, Grant/Award Number: 18H02774, 21K07230 and 21K07688

## Abstract

Synovial sarcomas are rare tumors arising in adolescents and young adults. The prognosis for advanced disease is poor, with an overall survival of 12-18 months. Frizzled homolog 10 (FZD10) is overexpressed in most synovial sarcomas, making it a promising therapeutic target. The results of a phase 1 trial of  $\beta$ -radioimmunotherapy (RIT) with the  $^{90}\text{Y}$ -labeled anti-FZD10 antibody OTSA101 revealed a need for improved efficacy. The present study evaluated the potential of  $\alpha$ -RIT with OTSA101 labeled with the  $\alpha$ -emitter  $^{225}\text{Ac}$ . Competitive inhibition and cell binding assays showed that specific binding of  $^{225}\text{Ac}$ -labeled OTSA101 to SYO-1 synovial sarcoma cells was comparable to that of the imaging agent  $^{111}\text{In}$ -labeled OTSA101. Biodistribution studies showed high uptake in SYO-1 tumors and low uptake in normal organs, except for blood. Dosimetric studies showed that the biologically effective dose (BED) of  $^{225}\text{Ac}$ -labeled OTSA101 for tumors was 7.8 Bd higher than that of  $^{90}\text{Y}$ -labeled OTSA101.  $^{90}\text{Y}$ - and  $^{225}\text{Ac}$ -labeled OTSA101 decreased tumor volume and prolonged survival.  $^{225}\text{Ac}$ -labeled OTSA101 achieved a complete response in 60% of mice, and no recurrence was observed.  $^{225}\text{Ac}$ -labeled OTSA101 induced a larger amount of necrosis and apoptosis than  $^{90}\text{Y}$ -labeled OTSA101, although the cell proliferation decrease was comparable. The BED for normal organs and tissues was tolerable; no treatment-related mortality or obvious toxicity, except for temporary body weight loss, was observed.  $^{225}\text{Ac}$ -labeled OTSA101 provided a high BED for tumors and achieved a 60% complete response in the synovial sarcoma mouse model SYO-1. RIT with  $^{225}\text{Ac}$ -labeled OTSA101 is a promising therapeutic option for synovial sarcoma.

## KEYWORDS

barendsen unit, complete response, molecular radiotherapy, relative biological effect, therapeutic nuclear medicine

This is an open access article under the terms of the Creative Commons Attribution-NonCommercial License, which permits use, distribution and reproduction in any medium, provided the original work is properly cited and is not used for commercial purposes.

© 2021 The Authors. *Cancer Science* published by John Wiley & Sons Australia, Ltd on behalf of Japanese Cancer Association.

## 1 | INTRODUCTION

Synovial sarcoma is a rare tumor arising in adolescents and young adults, usually in the extremities.<sup>1</sup> Therapy for patients with localized disease is based on surgery followed by external radiotherapy.<sup>2</sup> The 5-year survival rates vary from 40% to 60%.<sup>3</sup> Recurrences may be local (30%-50%) or distant (40%), with the lungs being the most common site of distant metastases.<sup>3</sup> The standard therapy for advanced disease is systemic chemotherapy with doxorubicin and/or ifosfamide.<sup>2</sup> Median overall survival is 12-18 months.<sup>4</sup> More effective therapeutic options for advanced synovial sarcoma are therefore highly desired.

Frizzled homolog 10 (FZD10) is a transmembrane protein belonging to the Frizzled family.<sup>5</sup> It is overexpressed in most synovial sarcomas and absent or very low in normal adult tissues except for the placenta.<sup>6</sup> Therefore, FZD10 is a promising therapeutic target for synovial sarcoma. A preclinical study with an anti-FZD10 antibody radiolabeled with the  $\beta$ -emitter yttrium-90 (<sup>90</sup>Y) showed strong antitumor effects in a SYO-1 synovial sarcoma mouse model without significant toxicity.<sup>7</sup> These findings support the clinical development of an antibody targeting FZD10 as a specific tool for radionuclide delivery to synovial sarcoma cells. A phase 1 trial of the <sup>90</sup>Y-labeled anti-FZD10 antibody OTSA101 for synovial sarcoma patients was recently conducted.<sup>8</sup> Some of the enrolled patients showed a stable-disease response to the therapy for recurrent sarcomas. The development of new treatments is important to provide additional options to patients with stable disease.

The clinical efficacy of targeted radionuclide therapy with  $\alpha$ -particle emitters for solid cancer has been demonstrated.<sup>9</sup>  $\alpha$ -Particle emitters have a greater linear energy transfer than  $\beta$ -emitters and deposit more energy to tumor cells (Figure S1).<sup>10</sup> A previous preclinical study demonstrated that the  $\alpha$ -emitting astatine-211 (<sup>211</sup>At)-labeled antibody OTSA101 had marked antitumor effects in the synovial sarcoma mouse model SYO-1 but did not achieve a complete response.<sup>11</sup> Actinium-225 (<sup>225</sup>Ac) is an  $\alpha$ -emitting radionuclide that generates a total of four  $\alpha$ -particles in the decay chain.<sup>12</sup> The half-life of <sup>225</sup>Ac is longer than that of <sup>211</sup>At and more appropriate for the pharmacokinetics of antibodies, therefore FZD10-targeted radioimmunotherapy (RIT) with <sup>225</sup>Ac is expected to have higher efficacy.

In the present study, we first evaluated the effect of <sup>225</sup>Ac labeling on binding of the anti-FZD10 antibody OTSA101 to SYO-1 synovial sarcoma cells. A biodistribution study of <sup>111</sup>In-labeled OTSA101 was conducted in SYO-1 tumor-bearing mice. The absorbed doses of <sup>90</sup>Y- and <sup>225</sup>Ac-labeled OTSA101 were estimated on the basis of the biodistribution data. Finally, the antitumor effects of <sup>90</sup>Y- and <sup>225</sup>Ac-labeled OTSA101 were assessed in the SYO-1 mouse model and histologic analysis was conducted.

## 2 | MATERIALS AND METHODS

### 2.1 | Antibody

The humanized chimeric antibody OTSA101, which recognizes human FZD10 but not murine FZD10, was provided by OncoTherapy

Science, Inc. As a control, human IgG<sub>1</sub> was purchased from Millipore Sigma.

### 2.2 | Cell culture

A human synovial sarcoma cell line, SYO-1, was gifted from Dr A. Kawai (National Cancer Center, Tokyo, Japan). The cells were cultured in DMEM (FUJIFILM Wako Pure Chemical Corporation) containing 10% fetal bovine serum (Thermo Fisher Scientific Inc.) in 5% CO<sub>2</sub> at 37°C.

### 2.3 | Antibody radiolabeling

Antibodies were conjugated with *p*-SCN-Bn-DOTA (DOTA, Macrocyclics) as previously described.<sup>13</sup> Briefly, antibodies (5 mg/mL) were reacted with four equal molar amounts of DOTA in 50 mmol/L borate buffer (pH 8.5) for 16 hours at 37°C. The DOTA to antibody conjugation ratios were approximately 2.8 each as determined by radio-thin-layer chromatography (TLC) with 80% methanol. The DOTA-conjugated antibody was purified by elution with 0.1 mol/L acetate buffer (pH 6.0) using a Sephadex G-50 (GE Healthcare Bio-Sciences) column. <sup>111</sup>InCl<sub>3</sub> (Nihon Medi-Physics) or <sup>90</sup>YCl<sub>3</sub> (Perkin Elmer) was incubated in 0.5 mol/L acetate buffer (pH 6.0) for 5 minutes at room temperature. Each was mixed with the DOTA-antibody conjugate and incubated for 60 minutes at 37°C. Radiolabeling of the antibody with <sup>225</sup>Ac was conducted as described previously.<sup>14</sup> <sup>225</sup>AcNO<sub>3</sub> (Oak Ridge National Labs) dissolved in 200 mmol/L UltraPur™ HCl (Kanto Chemical Co., Inc.) was added to 2 mol/L tetramethylammonium acetate (Tokyo Chemical Industry) and 150 g/L L-ascorbic acid (Millipore Sigma). DOTA-conjugated antibody was added and the mixture was incubated for 60 minutes at 37°C. The radiolabeled antibody was purified using an Amicon Ultra centrifugal filter (Merck Millipore) and the purified antibody was analyzed by radio-TLC. The specific activities were 7.8 ± 1.6 kBq/μg for <sup>111</sup>In-labeled OTSA101, 10.5 ± 5.4 kBq/μg for the <sup>111</sup>In-labeled control antibody, 518.4 ± 37.6 kBq/μg for <sup>90</sup>Y-labeled OTSA101, 481.1 kBq/μg for the <sup>90</sup>Y-labeled control antibody, 0.6 ± 0.4 kBq/μg for <sup>225</sup>Ac-labeled OTSA101, and 0.6 ± 0.3 kBq/μg for the <sup>225</sup>Ac-labeled control antibody. The radiochemical yields were 80.1 ± 18.3% for <sup>111</sup>In-labeled OTSA101, 91.0 ± 5.2% for the <sup>111</sup>In-labeled control antibody, 93.4 ± 5.8% for <sup>90</sup>Y-labeled OTSA101, 90.2% for the <sup>90</sup>Y-labeled control antibody, 31.3 ± 14.4% for <sup>225</sup>Ac-labeled OTSA101, and 33.1 ± 10.1% for the <sup>225</sup>Ac-labeled control antibody. The radiochemical purities were greater than 96% after purification.

### 2.4 | Cell binding and competitive inhibition assays

For the competitive inhibition assays, SYO-1 cells (2.0 × 10<sup>7</sup>) in phosphate-buffered saline with 1% BSA (Millipore Sigma) were incubated with <sup>111</sup>In-labeled antibodies in the presence of varying

concentrations of intact OTSA101, DOTA-conjugated OTSA101, or control antibody (0, 0.02, 0.07, 0.2, 0.7, 2.0, 6.1, 18.2, and 54.5 nmol/L) on ice for 60 minutes. After washing, cell-bound radioactivity was measured with a gamma counter (Wizard2 Automatic Gamma Counter, PerkinElmer). The dissociation constant was estimated by applying data to a one-site competitive binding model using GraphPad Prism 8 software (GraphPad Software).

For the cell binding assays, SYO-1 cells ( $2.0 \times 10^7$ ) in phosphate-buffered saline with 1% BSA were incubated with  $^{111}\text{In}$  and  $^{225}\text{Ac}$ -labeled antibodies on ice for 60 minutes. After washing, cell-bound radioactivity was measured using a gamma-counter with an energy window of 150-350 keV for  $^{111}\text{In}$  and 200-300 keV for  $^{225}\text{Ac}$  (Wizard2 Automatic Gamma Counter).

## 2.5 | Tumor model

The animal experimental protocol was approved by the Animal Care and Use Committee of the National Institutes for Quantum and Radiological Science and Technology (13-1022, 26 May 2016), and all animal experiments were conducted following the Guidelines regarding Animal Care and Handling. SYO-1 cells ( $5 \times 10^6$ ) were subcutaneously inoculated into male nude mice (BALB/c-nu/nu, 4 weeks old; CLEA Japan) under isoflurane anesthesia.

## 2.6 | Biodistribution of radiolabeled antibody

When tumor volumes reached approximately  $100 \text{ mm}^3$ , mice ( $n = 5$ /time-point), were intravenously injected with  $^{111}\text{In}$ -labeled antibodies (37 kBq) in a total of 30  $\mu\text{g}$  of antibody adjusted by adding the intact antibody. The mice were killed by isoflurane inhalation on days 1, 2, 4, or 7 after injection of  $^{111}\text{In}$ -labeled antibodies. Blood was obtained from the heart, and the tumor, lung, liver, spleen, pancreas, intestine, kidney, muscle, and bone were dissected and weighed. Radioactivity was measured with a gamma counter (PerkinElmer). Uptake is represented as the percentage of injected dose (radioactivity) per gram of tissue (% ID/g).

## 2.7 | Dosimetry

As described previously,<sup>13,15</sup> the absorbed doses of  $^{90}\text{Y}$ - and  $^{225}\text{Ac}$ -labeled antibodies were estimated using the area under the curve based on the biodistribution data of  $^{111}\text{In}$ -labeled antibodies and the mean energy emitted per transition of  $^{90}\text{Y}$ ,  $1.495 \times 10^{-13} \text{ Gy kg (Bq s)}^{-1}$ , and  $^{225}\text{Ac}$ , and all the daughter nuclei with corrections for branching,  $4.6262 \times 10^{-12} \text{ Gy kg (Bq s)}^{-1}$ .<sup>16</sup> The bone marrow absorbed dose was based on the blood data, considering a red marrow-to-blood activity ratio of 0.4.<sup>17</sup> Radiation weighting factors of 1 and 5 were used for  $^{90}\text{Y}$  and  $^{225}\text{Ac}$ , respectively, as recommended by the

Medical Internal Radiation Dose Committee.<sup>18</sup> This biologically effective dose (BED) is expressed in barendsen (Bd).<sup>19</sup>

## 2.8 | Radioimmunotherapy with $^{90}\text{Y}$ - and $^{225}\text{Ac}$ -labeled antibodies

The mice were intravenously injected with intact OTSA101 (0 MBq,  $n = 5$ ),  $^{90}\text{Y}$ -labeled control antibody (1.85 MBq,  $n = 5$ ),  $^{225}\text{Ac}$ -labeled control antibody (0.01 MBq,  $n = 5$ ),  $^{90}\text{Y}$ -labeled OTSA101 (1.85 MBq,  $n = 5$ ), or  $^{225}\text{Ac}$ -labeled OTSA101 (0.01 MBq,  $n = 5$ ) in a total of 30  $\mu\text{g}$  of antibody adjusted by adding the corresponding unlabeled antibody. Tumor sizes and body weights were measured at least twice a week for 4 weeks after administration. Tumor size was measured using a digital caliper, and the tumor volume was calculated according to the following formula: tumor volume ( $\text{mm}^3$ ) = (length  $\times$  width<sup>2</sup>)/2. When the tumor volume reached more than  $800 \text{ mm}^3$  and body weight loss was more than 20% compared with that at day 0, the mouse was humanely killed by isoflurane inhalation.

## 2.9 | Histologic analysis

SYO-1 tumors were resected from mice on days 1, 3, or 7 after injection with intact OTSA101 (0 MBq,  $n = 3$ /time-point),  $^{90}\text{Y}$ -labeled OTSA101 (1.85 MBq,  $n = 3$ /time-point), or  $^{225}\text{Ac}$ -labeled OTSA101 (0.01 MBq,  $n = 3$ /time-point). The tumors were fixed in 10% neutral-buffered formalin, embedded in paraffin, and cut into 1- $\mu\text{m}$  thick sections. The tumor sections were deparaffinized and stained with H&E. CD3 positive lymphocytes were detected by immunohistochemical staining with a rabbit anti-CD3 antibody (SP7; Abcam). Tumor cell proliferation was evaluated by Ki-67 immunohistochemical staining with a rabbit anti-Ki-67 antibody (SP6; Abcam), and an anti-rabbit HRP/DAB Detection kit (Abcam). The Ki-67 index was calculated by counting the percentage of Ki-67-positive tumor cells per >2500 tumor cells in a section with 200 $\times$  magnification ( $n = 3$ ). Apoptosis was detected using the DeadEnd Colorimetric TUNEL System (Promega).

## 2.10 | Statistical analysis

Data are expressed as the means  $\pm$  standard deviation. Statistical analysis was performed using GraphPad Prism 8 software. Tumor volume data were analyzed by two-way ANOVA. Ki-67 staining data were analyzed by one-way ANOVA with Tukey's multiple comparison test. Uptake data of radiolabeled antibodies were analyzed by unpaired *t* test. Log-rank tests were used to evaluate Kaplan-Meier survival curves based on the endpoint of tumor volume of  $300 \text{ mm}^3$ . A *P* value <.05 was considered statistically significant in all experiments.

### 3 | RESULTS

#### 3.1 | In vitro antibody characterization

The competitive inhibition assay provided estimated binding affinities ( $K_d$ ) of intact OTSA101 and DOTA-conjugated OTSA101 of 1.6 and 1.7 nmol/L, respectively (Figure 1A), suggesting that the chelate conjugation procedure had a limited effect on affinity. The control antibody did not inhibit the binding of  $^{111}\text{In}$ -labeled OTSA101 to SYO-1 cells (Figure 1B). Cell binding assays with SYO-1 showed no significant difference between  $^{111}\text{In}$ - and  $^{225}\text{Ac}$ -labeled OTSA101 (Figure 1C). No  $^{111}\text{In}$ - and  $^{225}\text{Ac}$ -labeled control antibodies bound to the SYO-1 cells (Figure 1D).

#### 3.2 | Biodistribution of $^{111}\text{In}$ -labeled antibodies in nude mice bearing SYO-1 tumors

Tumor uptake of  $^{111}\text{In}$ -labeled OTSA101 was significantly higher than that of the  $^{111}\text{In}$ -labeled control antibody ( $P < .01$  at days 2 and 4,  $P < .05$  at day 7; Table 1). The maximum tumor uptake of  $^{111}\text{In}$ -labeled OTSA101 was  $24.8 \pm 6.5\%$  ID/g at 4 days after injection. The uptake of  $^{111}\text{In}$ -labeled OTSA101 in the blood and lung was significantly higher than the uptake of the  $^{111}\text{In}$ -labeled control antibody ( $P < .01$  or  $P < .05$ ; Table 1), whereas the uptake of  $^{111}\text{In}$ -labeled OTSA101 into the liver and spleen was lower than of the  $^{111}\text{In}$ -labeled control antibody ( $P < .01$ ; Table 1). In

the other normal organs, there was no significant difference in the uptake of  $^{111}\text{In}$ -labeled control antibody and OTSA101 (Table 1).

#### 3.3 | Dosimetry

Based on the biodistribution studies, the absorbed doses were estimated when  $^{111}\text{In}$  was replaced with  $^{90}\text{Y}$  and  $^{225}\text{Ac}$ . Table 2 shows estimated absorbed doses when no radiation weighted factor was considered. The absorbed doses of radiolabeled OTSA101 in the lungs, bone marrow, and tumor were higher than that of the radiolabeled control antibody ( $P < .01$ ; Table 2). The doses of the radiolabeled OTSA101 in the liver and spleen were lower than those of the control antibody ( $P < .01$ ; Table 2).

For calculating a relative biological effect (RBE), the absorbed doses (Gy) from the treatment doses of  $^{90}\text{Y}$ - and  $^{225}\text{Ac}$ -labeled antibodies were calculated without considering a radiation weighted factor (Table 3). The dose absorbed by tumors treated with 1.85 MBq  $^{90}\text{Y}$ -labeled OTSA101 was 3.1-fold higher than that with 0.01 MBq  $^{225}\text{Ac}$ -labeled OTSA101 (Table 3).

Regarding the efficacy and safety, the BED (Bd) considering radiation weighting factors of 1 for  $^{90}\text{Y}$  and 5 for  $^{225}\text{Ac}$  are shown in Table 4. The BED to bone marrow from 0.01 MBq  $^{225}\text{Ac}$ -labeled OTSA101 was 1.3-fold higher than that from 1.85 MBq  $^{90}\text{Y}$ -labeled OTSA101 (Table 4). The doses to organs were higher when injected with  $^{225}\text{Ac}$ -labeled OTSA101 than with  $^{90}\text{Y}$ -labeled

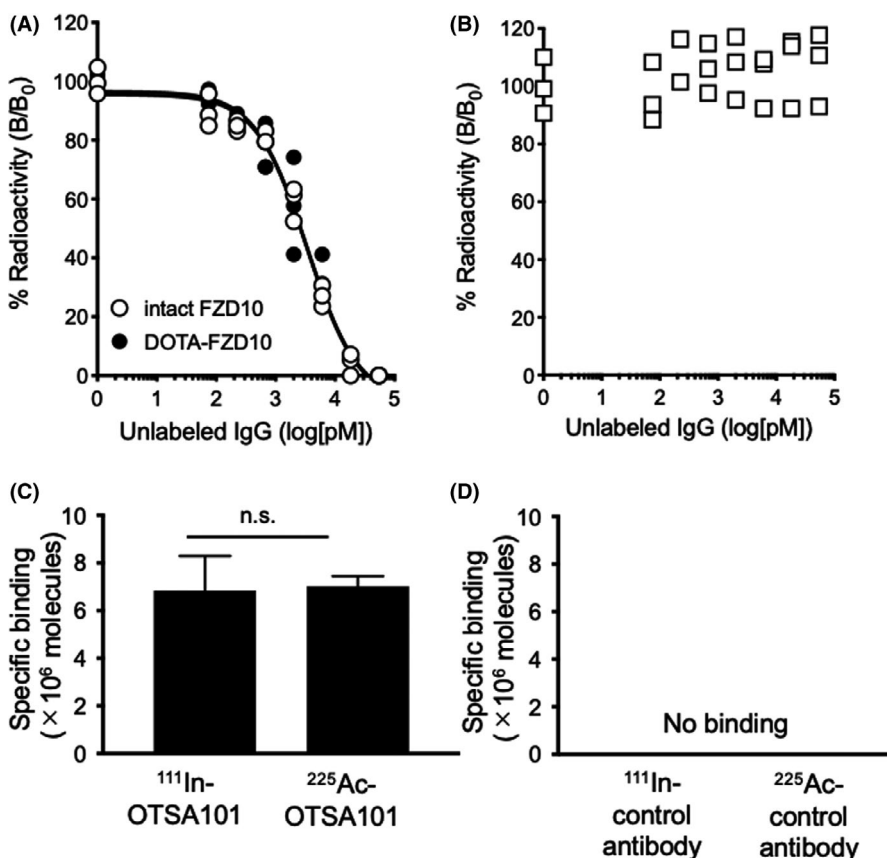


**FIGURE 1** In vitro characterization of radiolabeled OTSA101. A, Competitive inhibition assay for intact OTSA101 (white circles) and DOTA-conjugated OTSA101 (black circles) with SYO-1 cells. B, Competitive inhibition assay for the control antibody. C, Cell binding assay of  $^{111}\text{In}$ - and  $^{225}\text{Ac}$ -labeled OTSA101. Data represent the mean + standard deviation. D, Cell binding assay of the  $^{111}\text{In}$ - and  $^{225}\text{Ac}$ -labeled control antibodies

**TABLE 1** Biodistribution of  $^{111}\text{In}$ -labeled antibodies in SYO-1 tumor-bearing mice

	Day 1	Day 2	Day 4	Day 7
Control antibody				
Blood	12.1 ± 1.2	7.6 ± 1.3	5.3 ± 2.5	3.1 ± 0.7
Lung	5.7 ± 0.7	3.5 ± 0.8	3.6 ± 1.1	2.2 ± 0.5
Liver	12.6 ± 0.7	10.4 ± 1.0	10.0 ± 1.8	7.5 ± 1.0
Spleen	8.1 ± 0.5	7.2 ± 1.1	7.1 ± 1.1	5.9 ± 1.0
Pancreas	5.4 ± 8.0	1.5 ± 0.2	1.5 ± 0.3	1.2 ± 0.1
Intestine	2.2 ± 0.8	1.8 ± 0.3	1.1 ± 0.3	0.6 ± 0.1
Kidney	13.5 ± 0.8	11.2 ± 2.0	8.0 ± 1.7	5.4 ± 0.8
Muscle	1.1 ± 0.9	0.9 ± 0.6	0.7 ± 0.2	0.5 ± 0.1
Tumor	8.3 ± 2.0	8.1 ± 3.7	7.3 ± 3.0	7.6 ± 2.9
OTSA101				
Blood	21.6 ± 3.1**	14.9 ± 0.9**	10.1 ± 3.6 <sup>†</sup>	4.3 ± 2.0
Lung	7.8 ± 1.0**	5.6 ± 0.7**	4.1 ± 1.8	2.4 ± 1.1
Liver	7.2 ± 0.6**	5.8 ± 0.7**	5.0 ± 0.7**	3.9 ± 0.5**
Spleen	5.6 ± 0.8**	5.5 ± 0.3 <sup>†</sup>	5.2 ± 0.6 <sup>†</sup>	3.6 ± 0.5 <sup>†</sup>
Pancreas	2.3 ± 0.2	1.9 ± 0.2	1.2 ± 0.2	0.6 ± 0.2
Intestine	2.1 ± 0.2	1.9 ± 0.3	1.2 ± 0.2	0.6 ± 0.2
Kidney	13.1 ± 1.9	9.4 ± 0.7	5.8 ± 1.4	3.2 ± 0.6**
Muscle	1.3 ± 0.2	1.2 ± 0.1	0.8 ± 0.2	0.6 ± 0.2
Tumor	12.1 ± 3.8	21.3 ± 3.1**	24.8 ± 6.5**	17.3 ± 6.1 <sup>†</sup>

Note: Data indicate as the percentage of injected dose per gram (%ID/g) and as the mean ± standard deviation.

\* $P < .05$ ; \*\* $P < .01$ .

**TABLE 2** Estimated absorbed dose (Gy/MBq) of  $^{90}\text{Y}$ - and  $^{225}\text{Ac}$ -labeled antibodies based on the biodistribution data of  $^{111}\text{In}$ -labeled antibodies, not considering a radiation weighting factor

	$^{90}\text{Y}$		$^{225}\text{Ac}$	
	Control antibody	OTSA101	Control antibody	OTSA101
Lung	1.5 ± 0.1	2.0 ± 0.1**	74.9 ± 4.7	98.3 ± 6.9**
Liver	3.8 ± 0.1	2.1 ± 0.1**	205.0 ± 8.7	108.9 ± 4.1**
Spleen	2.6 ± 0.1	1.9 ± 0.1**	143.5 ± 8.7	101.8 ± 7.4**
Pancreas	0.9 ± 0.4	0.6 ± 0.0	44.1 ± 13.5	31.9 ± 2.5
Intestine	0.6 ± 0.0	0.7 ± 0.1	28.2 ± 1.7	32.7 ± 3.5**
Kidney	3.7 ± 0.3	3.3 ± 0.2 <sup>†</sup>	189.8 ± 12.2	161.6 ± 10.6**
Muscle	0.3 ± 0.0	0.4 ± 0.1	16.3 ± 0.9	22.1 ± 3.1**
Bone marrow <sup>a</sup>	1.1 ± 0.1	2.1 ± 0.1**	54.4 ± 3.8	100.3 ± 5.5**
Tumor	2.8 ± 0.3	7.0 ± 0.4**	159.0 ± 65.9	408.3 ± 184.7**

Note: Data indicate the mean ± standard deviation.

<sup>a</sup>Absorbed doses of bone marrow were estimated based on the blood uptake (Table 1), considering a red marrow-to-blood activity ratio of 0.4.

\*\* $P < .01$ ; \* $P < .05$  vs control.

OTSA101 (Table 4). The BED to tumors from  $^{90}\text{Y}$ - and  $^{225}\text{Ac}$ -labeled control antibodies was lower than that from  $^{90}\text{Y}$ -labeled OTSA101 (Table 4). The doses to some organs such as the liver and spleen from radiolabeled control antibodies were higher than that from radiolabeled OTSA101 (Table 4) because the tumor uptake of the control antibodies was lower, leading to higher uptake in normal organs.

### 3.4 | Treatment effects of radiolabeled antibodies in nude mice bearing SYO-1 tumors

The tumors in mice injected with intact OTSA101, and  $^{90}\text{Y}$ - and  $^{225}\text{Ac}$ -labeled control antibodies rapidly increased in size (Figure 2A). In mice treated with  $^{90}\text{Y}$ - and  $^{225}\text{Ac}$ -labeled OTSA101, marked antitumor effects were observed ( $P < .01$ , vs intact OTSA101, and  $^{90}\text{Y}$ - and  $^{225}\text{Ac}$ -labeled

	1.85 MBq <sup>90</sup> Y-control antibody	1.85 MBq <sup>90</sup> Y-OTSA101	0.01 MBq <sup>225</sup> Ac-control antibody	0.01 MBq <sup>225</sup> Ac-OTSA101
Lung	2.7	3.6	0.8	1.0
Liver	7.1	3.8	2.1	1.1
Spleen	4.9	3.5	1.5	1.0
Pancreas	1.7	1.1	0.5	0.3
Intestine	1.1	1.2	0.3	0.3
Kidney	6.9	6.2	1.9	1.6
Muscle	0.6	0.8	0.2	0.2
Bone marrow <sup>a</sup>	2.1	3.8	0.6	1.0
Tumor	5.2	13.0	1.6	4.2

<sup>a</sup>Absorbed doses of bone marrow were estimated based on the blood uptake (Table 1), considering a red marrow-to-blood activity ratio of 0.4.

	1.85 MBq <sup>90</sup> Y-control antibody	1.85 MBq <sup>90</sup> Y-OTSA101	0.01 MBq <sup>225</sup> Ac-control antibody	0.01 MBq <sup>225</sup> Ac-OTSA101
Lung	2.7	3.6	3.8	5.0
Liver	7.1	3.8	10.5	5.6
Spleen	4.9	3.5	7.3	5.2
Pancreas	1.7	1.1	2.3	1.6
Intestine	1.1	1.2	1.4	1.7
Kidney	6.9	6.2	9.7	8.2
Muscle	0.6	0.8	0.8	1.1
Bone marrow <sup>b</sup>	2.1	3.8	2.8	5.1
Tumor	5.2	13.0	8.1	20.8

<sup>a</sup>Radiation weighting factor of 1 for <sup>90</sup>Y and 5 for <sup>225</sup>Ac.

<sup>b</sup>Absorbed doses of bone marrow were estimated based on the blood uptake (Table 1), considering a red marrow-to-blood activity ratio of 0.4.

control antibodies; Figure 2A). In the group treated with <sup>90</sup>Y-OTSA101, the tumor size decreased in the first 14 days after injection and thereafter gradually increased in all the mice (Figure 2A). Treatment with <sup>225</sup>Ac-OTSA101 induced significant tumor reduction. Notably, the tumors disappeared in three of the five mice, and no regrowth was observed until the end of the study period (Figures 2A and S2).

Kaplan-Meier survival curves based on the endpoint of tumor volume of 300 mm<sup>3</sup> are shown in Figure 2B. Injection with <sup>90</sup>Y- and <sup>225</sup>Ac-labeled OTSA101 significantly prolonged survival compared with the intact and radiolabeled control antibody groups ( $P < .01$ ). No significant difference was detected between the two radiolabeled OTSA101 groups (Figure 2B).

None of the mice showed significant body weight loss (Figure S3A). No obvious damage from radiolabeled treatments was detected in the bone marrow of mice treated with <sup>90</sup>Y- or <sup>225</sup>Ac-labeled OTSA101 (Figure S3B).

### 3.5 | Histologic analysis of SYO-1 tumors treated with radiolabeled OTSA101

Tumors treated with intact OTSA101 showed biphasic features consisting of spindle cells and polygonal epithelial cells, and several

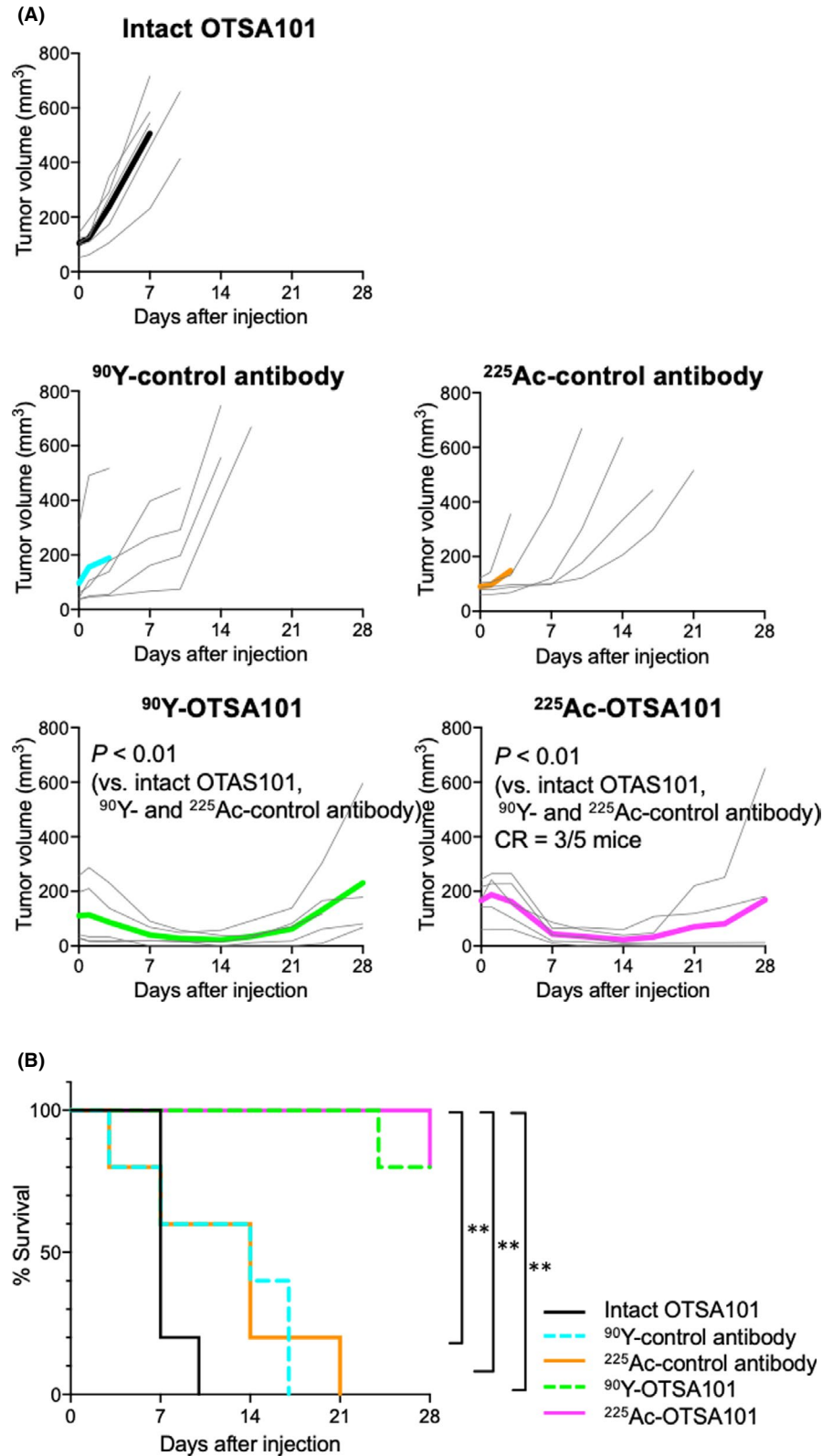
**TABLE 3** Estimated absorbed doses (Gy) from the treatment dose of <sup>90</sup>Y- and <sup>225</sup>Ac-labeled OTSA101, not considering a radiation weighting factor

**TABLE 4** Biologically effective doses (Bd) from the treatment dose of <sup>90</sup>Y- and <sup>225</sup>Ac-labeled OTSA101 using radiation weighting factors<sup>a</sup>

mitotic cells (Figure 3A, upper panels). These characteristics are consistent with previous observations.<sup>20</sup> In tumors treated with <sup>90</sup>Y-labeled OTSA101, necrosis and hemorrhage were observed on day 1, and tumor cellularity was decreased on day 3. On day 7, the tumor cells were further decreased and fibrous tissue was increased (Figure 3A, middle panels). Tumors treated with <sup>225</sup>Ac-OTSA101 showed more damage than those treated with <sup>90</sup>Y-labeled OTSA101. In tumors treated with <sup>225</sup>Ac-labeled OTSA101, tumor cell reduction was observed on days 1 and 3. On day 7, fibroblasts and fibrous tissue were observed instead of tumor cells (Figure 3A, lower panels). Treatment with <sup>90</sup>Y- and <sup>225</sup>Ac-labeled OTSA101 induced lymphocyte infiltration into the tumors on days 1 and 3 (Figure 3B). CD3-positive lymphocytes were observed more in tumors treated with <sup>225</sup>Ac-labeled OTSA101 compared with those with <sup>90</sup>Y-labeled OTSA101 (Figure 3B, middle and lower panels).

Treatment with <sup>90</sup>Y- and <sup>225</sup>Ac-labeled OTSA101 significantly reduced the number of proliferating (Ki-67-positive) tumor cells compared with tumors treated with intact OTSA101 ( $P < .01$ ; Figure 4A,B). Apoptotic cells were observed on day 3 in tumors treated with <sup>90</sup>Y- and <sup>225</sup>Ac-labeled OTSA101 (Figure 5). <sup>225</sup>Ac-labeled OTSA101 induced a relatively greater amount of apoptosis than <sup>90</sup>Y-labeled OTSA101 (Figure 5). No apoptosis was observed in tumors treated with intact OTSA101 (Figure 5).

**FIGURE 2** Therapeutic efficacy of  $^{90}\text{Y}$ - and  $^{225}\text{Ac}$ -labeled antibodies in SYO-1 tumor-bearing mice. A, Tumor growth curves in each mouse after injection with intact OTSA101 and  $^{90}\text{Y}$ - and  $^{225}\text{Ac}$ -labeled antibodies (thin lines). Bold lines indicate the mean. CR, complete response. B, Kaplan-Meier survival curves based on an endpoint of tumor volume  $\geq 300 \text{ mm}^3$ . \*\* $P < .01$



## 4 | DISCUSSION

Treatments with  $^{90}\text{Y}$ - and  $^{225}\text{Ac}$ -labeled OTSA101 provided strong antitumor effects in the synovial sarcoma mouse model SYO-1.  $^{90}\text{Y}$ - and  $^{225}\text{Ac}$ -labeled OTSA101 decreased tumor volume and prolonged survival. Although there was no statistically significant

difference in the tumor suppression or survival prolongation between the two treatments, only  $^{225}\text{Ac}$ -labeled OTSA101 induced tumor disappearance (complete response) in 60% of mice, and recurrence was not observed through the end of the study. To our knowledge, this represents the best response in FZD10-targeted RIT to date. Pathologic analysis revealed that  $^{225}\text{Ac}$ -labeled

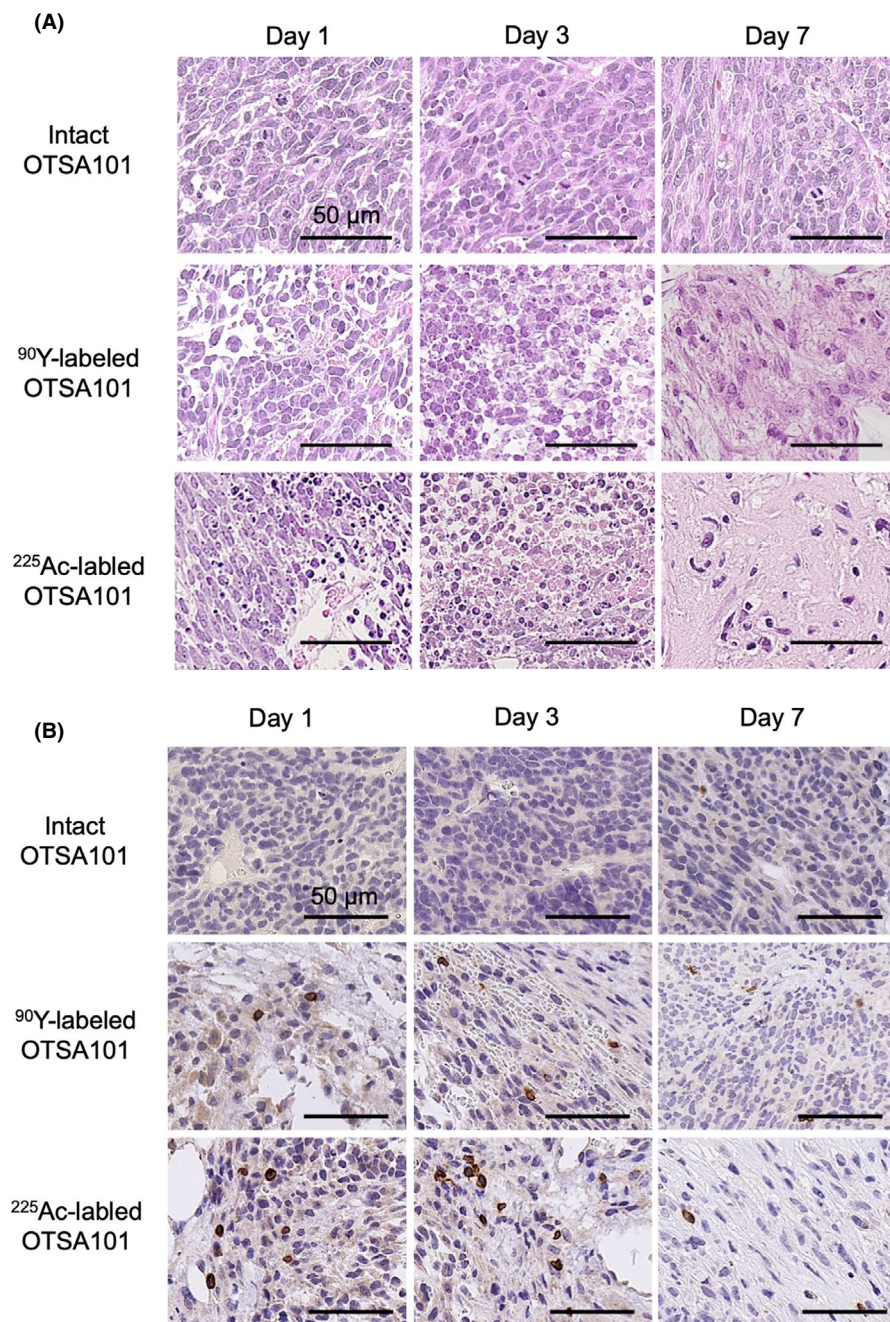


**FIGURE 3** A, H&E-stained sections of SYO-1 tumors treated with intact, <sup>90</sup>Y-labeled OTSA101, and <sup>225</sup>Ac-labeled OTSA101 on days 1, 3, and 7 after injection. B, CD3-positive lymphocytes in SYO-1 tumors treated with intact OTSA101, <sup>90</sup>Y-labeled OTSA101, and <sup>225</sup>Ac-labeled OTSA101 at days 1, 3, and 7 after injection. Bars, 50  $\mu$ m

OTSA101 induced more necrotic and apoptotic tumor cells compared with <sup>90</sup>Y-labeled OTSA101, likely because <sup>225</sup>Ac-labeled OTSA101 irradiated the tumors with 7.8-Bd higher BED compared with <sup>90</sup>Y-labeled OTSA101 (20.8 Bd<sub>RBE5</sub> vs 13.0 Bd<sub>RBE1</sub>). In addition,  $\alpha$ -emitters damage cells to a greater extent than  $\beta$ -emitters.<sup>21</sup> Previous reports have shown FZD10 expression in SYO-1 tumors<sup>22</sup> and synovial sarcoma specimens.<sup>6,7</sup> The expression seems to be similar between them, although it has not been directly compared. RIT with <sup>225</sup>Ac-labeled OTSA101 is another promising option for advanced synovial sarcoma showing a limited response to <sup>90</sup>Y-labeled OTSA101 therapy. High FZD10 expression is also found in colorectal cancer<sup>23</sup>; FZD10-targeted  $\alpha$ -RIT with <sup>225</sup>Ac-labeled OTSA101 may be applicable for the treatment of colorectal cancer

with metastasis. Further preclinical studies in such cancer models are required.

Compared with a previous preclinical study with  $\alpha$ -emitting <sup>211</sup>At-labeled OTSA101 in the same mouse model,<sup>11</sup> <sup>225</sup>Ac-labeled OTSA101 showed a greater antitumor effect in the present study. <sup>225</sup>Ac-labeled OTSA101 provides a higher radiation dose to the tumors than <sup>211</sup>At-labeled OTSA101 (20.8 Bd<sub>RBE5</sub> vs 16.6 Bd<sub>RBE5</sub>). This difference is likely due to the difference in the half-life (10 days for <sup>225</sup>Ac vs 7 hours for <sup>211</sup>At).<sup>10</sup> Antibodies slowly penetrate tumor tissues,<sup>24</sup> and the longer half-life of <sup>225</sup>Ac is more suitable for RIT. In addition, the radiometal <sup>225</sup>Ac is retained longer in cells after internalization, resulting in a higher tumor accumulation of <sup>225</sup>Ac compared with the radiohalogen <sup>211</sup>At. These favorable properties of



**FIGURE 4** Tumor cell proliferation analysis using Ki-67 immunostaining. A, Ki-67-stained SYO-1 tumors on days 1, 3, and 7 after injection with intact,  $^{90}\text{Y}$ -labeled OTSA101, and  $^{225}\text{Ac}$ -labeled OTSA101. Bars, 50  $\mu\text{m}$ . B, Quantification of proliferating (Ki-67 positive) cells. Data represent the mean  $\pm$  standard deviation.  $**P < .01$

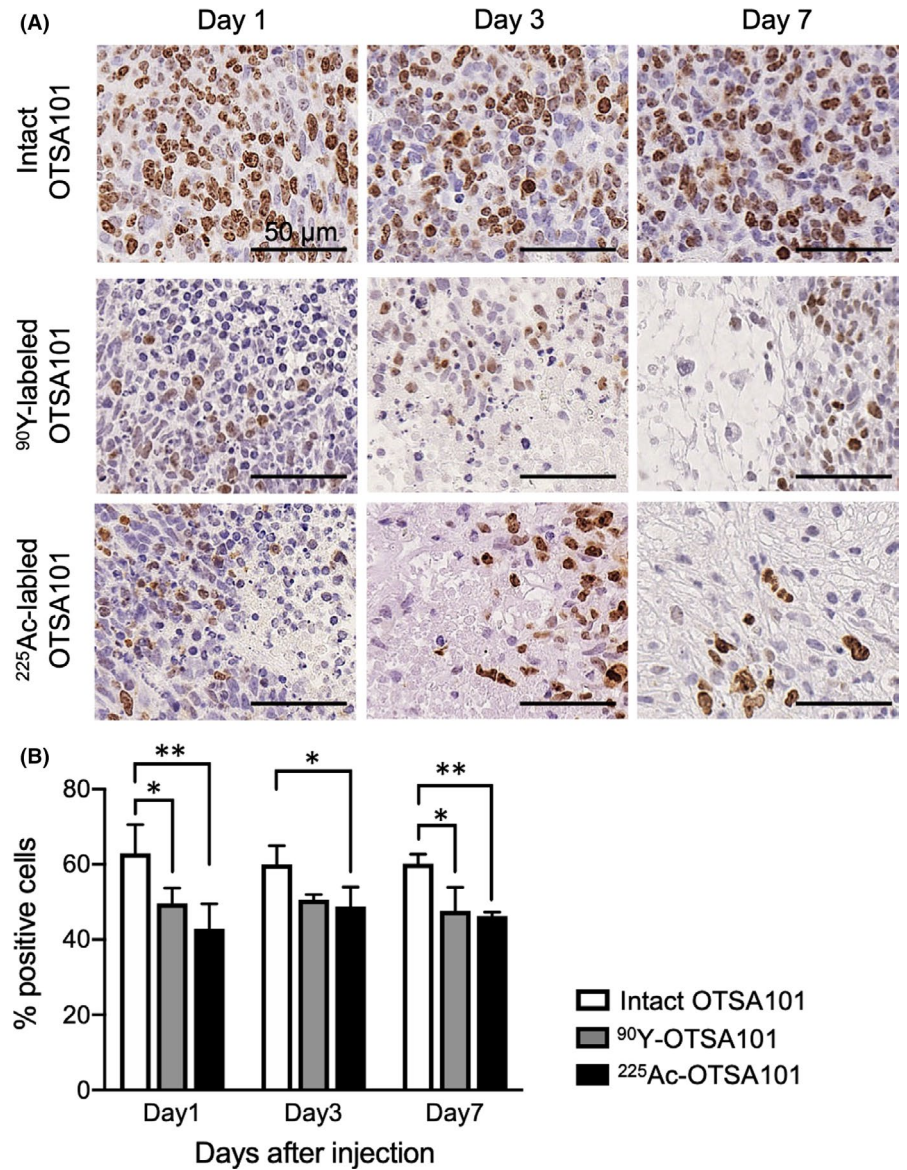
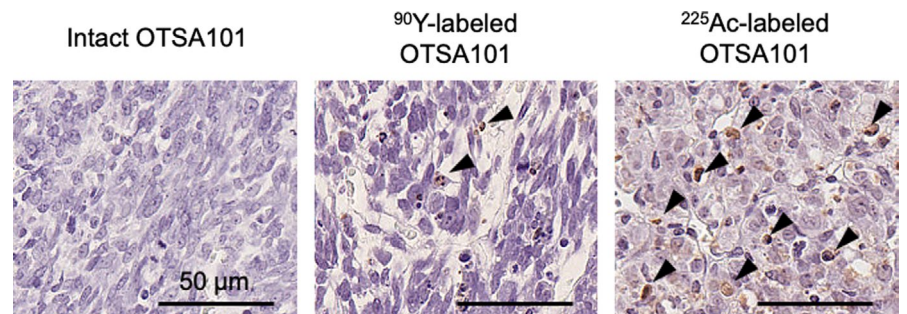


**FIGURE 5** Apoptotic analysis. TUNEL-stained SYO-1 tumors on day 3 after injection with intact OTSA101,  $^{90}\text{Y}$ -labeled OTSA101, and  $^{225}\text{Ac}$ -labeled OTSA101. Arrowheads indicate TUNEL-positive cells. Bar, 50  $\mu\text{m}$



$^{225}\text{Ac}$  led to a 60% complete response in mice treated with  $^{225}\text{Ac}$ -labeled OTSA101.

Interestingly, the present study found that  $^{225}\text{Ac}$ - and  $^{90}\text{Y}$ -labeled OTSA101 induced more apoptotic cells in the SYO-1 model compared with other cancer models treated with radionuclide therapy targeting different antigens.<sup>13,25,26</sup> RIT with  $\alpha$ - or  $\beta$ -emitters alone hardly induces a larger amount of apoptosis. FZD10 is in the Wnt signal pathway, and some Wnt inhibitors induce

apoptosis.<sup>6</sup> Intratumoral injections of the anti-FZD10 polyclonal antibody TT641 into nude mice induced apoptosis but did not decrease tumor volume.<sup>6</sup> FZD10 blockade with radiation from radio-labeled OTSA101 could enhance apoptosis induction and tumor volume reduction.

Regarding the clinical role of  $^{225}\text{Ac}$ - and  $^{90}\text{Y}$ -labeled OTSA101, each has a different therapeutic role in patients although the present study showed a higher antitumor effect of  $^{225}\text{Ac}$ -labeled OTSA101

compared with  $^{90}\text{Y}$ -labeled OTSA101. In clinical practice, the tumors are larger than those treated in the present preclinical study ( $\sim 100\text{ mm}^3$ ). The path length of  $\alpha$ -ray radiation from  $^{225}\text{Ac}$  is 47–85  $\mu\text{m}$ <sup>18</sup> and the antibody penetration in tissues is low,<sup>24</sup> therefore  $\alpha$ -RIT would produce a limited response in large tumors.<sup>27</sup> The  $\beta$ -ray radiation produced by  $^{90}\text{Y}$  has a maximum path length of 11 mm,<sup>28</sup> which is more suitable for treating large tumors. Thus, combined therapy with  $^{225}\text{Ac}$ -labeled OTSA101 and  $^{90}\text{Y}$ -labeled OTSA101 should be considered. Several reports of such combination therapy in clinical studies that provided a safely enhanced response were recently reviewed.<sup>29</sup> Further studies are needed to evaluate the therapeutic efficacy of RIT using  $^{225}\text{Ac}$ -labeled OTSA101 in combination with  $^{90}\text{Y}$ -labeled OTSA101.

Generally, monotherapy alone cannot cure aggressive tumors. Combination strategies are needed to improve the antitumor effect of RIT for refractory synovial sarcoma. Combination therapy utilizing an immune checkpoint blocking agent is a good candidate. Several clinical studies of soft tissue sarcomas including synovial sarcoma have been conducted, and programmed cell death protein 1 (PD-1) blockade combined with external-beam radiotherapy demonstrated promising results.<sup>30</sup> Radiation upregulates programmed death ligand 1 (PD-L1) expression in soft tissue sarcoma, even in patients with no tumor cell PD-L1 expression prior to radiotherapy.<sup>30</sup>  $\alpha$ -Irradiation of tumors has the potential to promote an antitumor immune response.<sup>31</sup> Taken together, combination therapy with PD-1 blockade might enhance the therapeutic effect of RIT with  $^{225}\text{Ac}$ -labeled OTSA101. Further studies are necessary to determine the possible clinical application of  $^{225}\text{Ac}$ -labeled OTSA101 for advanced stage synovial sarcoma.

In the present study, we applied a radiation weighting factor of 5 for calculating the BED of  $^{225}\text{Ac}$ -labeled OTSA101. It is important to assess whether or not this radiation weighting factor is appropriate before discussing the safety of treatment with  $^{225}\text{Ac}$ -labeled OTSA101. A dosimetric study based on the biodistribution of  $^{111}\text{In}$ -labeled OTSA101 showed that tumors absorbed doses of 13.0 Gy for  $^{90}\text{Y}$ -labeled OTSA101 and 4.2 Gy for  $^{225}\text{Ac}$ -labeled OTSA101, indicating that the RBE of  $^{225}\text{Ac}$ -labeled OTSA101 is 3.1. This is consistent with an RBE of 3 to 5 based on previous *in vivo* experiments.<sup>18,25</sup> The Medical Internal Radiation Dose Committee recommends an RBE of 5 for discussing safety,<sup>18</sup> therefore the BEDs shown in Table 4 based on a radiation weighting factor of 5 are appropriate. We discuss the safety based on this BED below.

Bone marrow is generally the dose-limiting tissue in RIT.<sup>21</sup> The dose to bone marrow was 3.8  $\text{Bd}_{\text{RBE1}}$  for  $^{90}\text{Y}$ -labeled OTSA101 and 5.1  $\text{Bd}_{\text{RBE5}}$  for  $^{225}\text{Ac}$ -labeled OTSA101. In rodents, the limiting absorbed doses in bone marrow are 6–9  $\text{Bd}$ ,<sup>32</sup> therefore the absorbed doses by  $^{90}\text{Y}$ - and  $^{225}\text{Ac}$ -labeled OTSA101 is acceptable in rodents. As expected, we observed no treatment-related mortality and bone marrow toxicity. For  $\beta$ -RIT in humans, however, the limiting dose to bone marrow is 2–4.5  $\text{Bd}$ .<sup>17,33,34</sup> The phase 1 trial for  $^{90}\text{Y}$ -labeled OTSA101 showed that the therapy was well-tolerated but grade 3

lymphopenia was observed in 80% of patients in which the estimated dose was approximately 2  $\text{Bd}$ .<sup>8</sup> The therapeutic radioactive dose of  $^{225}\text{Ac}$ -labeled OTSA101 needs to be determined considering this finding, but a decreased risk of hematotoxicity from  $^{225}\text{Ac}$ -labeled OTSA101 is expected compared with  $^{90}\text{Y}$ -labeled antibodies because of the short path lengths of  $\alpha$ -emitters.<sup>21</sup> Other organs with high absorbed doses, such as the liver, spleen, and kidneys, would tolerate the therapy because the doses were lower than their limiting doses in humans.<sup>35</sup> Overall,  $^{225}\text{Ac}$ -labeled OTSA101 would likely be tolerable, similar to  $^{90}\text{Y}$ -labeled OTSA101, in clinical settings.

There is no data about secondary cancer with our radiolabeled OTSA101 to date. However, there is a report about the risk of secondary primary malignancy of the radioimmunotherapeutic pharmaceutical  $^{90}\text{Y}$ -labeled Zevalin for non-Hodgkin lymphoma.<sup>36</sup> The follow-up analysis of 242 patients showed no difference in secondary cancer incidence between  $^{90}\text{Y}$ -labeled Zevalin and other therapy.<sup>36</sup> Unfortunately, there is no report of the risk of secondary cancer related to alpha-RIT. Further clinical studies are required to assess potential risks. However, absorbed doses of  $\alpha$ -RIT limited to the same dose of  $\beta$ -RIT would provide a similar risk of secondary cancer related to alpha-RIT.

The present study has several limitations. First, the observation period was only 4 weeks. It is important to follow up for a longer time to determine whether or not tumors recur. A longer observation might show differences in the therapeutic effects between  $^{90}\text{Y}$ - and  $^{225}\text{Ac}$ -labeled OTSA101. Second, the present study included a dosimetric study in animals, but no clinical dosimetry. The biodistribution of drugs, including antibodies, generally differs between humans and animals. Clinical dosimetric studies for  $^{225}\text{Ac}$ -labeled OTSA101 are needed to determine the safely injected radioactive doses for humans.

In conclusion,  $^{225}\text{Ac}$ -labeled OTSA101 provided a higher BED for tumors than  $^{90}\text{Y}$ -labeled OTSA101 and achieved a 60% complete response in the synovial sarcoma mouse model SYO-1. RIT with  $^{225}\text{Ac}$ -labeled OTSA101 is a promising therapeutic option for patients with synovial sarcoma.

## ACKNOWLEDGMENTS

We thank Yuriko Ogawa, Naoko Kuroda, and Akihito Abe for technical assistance and the staff in the Laboratory Animal Sciences section for animal management. This work was supported in part by JSPS KAKENHI 21K07688 (HS), 18H02774 (ABT), and 21K07230 (AS).

## DISCLOSURE

Yusuke Nakamura is a stockholder and scientific advisor at OncoTherapy Science, Inc. Toyomasa Katagiri is a stockholder and external board member at OncoTherapy Science, Inc. Yosuke Harada is a stockholder and employee at OncoTherapy Science, Inc. The other authors have no financial or other competing interests to declare in relation to this study.

## ORCID

Atsushi B. Tsuji  <https://orcid.org/0000-0003-2726-288X>

Toyomasa Katagiri  <https://orcid.org/0000-0001-5086-7444>

## REFERENCES

- Ducimetière F, Lurkin A, Ranchère-Vince D, et al. Incidence of sarcoma histotypes and molecular subtypes in a prospective epidemiological study with central pathology review and molecular testing. *PLoS One*. 2011;6:e20294.
- Spillane AJ, A'Hern R, Judson IR, Fisher C, Thomas JM. Synovial sarcoma: a clinicopathologic, staging, and prognostic assessment. *J Clin Oncol*. 2000;18:3794-3803.
- Canter RJ, Qin L-X, Maki RG, Brennan MF, Ladanyi M, Singer S. A synovial sarcoma-specific preoperative nomogram supports a survival benefit to ifosfamide-based chemotherapy and improves risk stratification for patients. *Clin Cancer Res*. 2008;14:8191-8197.
- Vlenterie M, Litiere S, Rizzo E, et al. Outcome of chemotherapy in advanced synovial sarcoma patients: review of 15 clinical trials from the European Organisation for Research and Treatment of Cancer Soft Tissue and Bone Sarcoma Group; setting a new landmark for studies in this entity. *Eur J Cancer*. 2016;58:62-72.
- Koike J, Takagi A, Miwa T, Hirai M, Terada M, Katoh M. Molecular cloning of Frizzled-10, a novel member of the Frizzled gene family. *Biochem Biophys Res Commun*. 1999;262:39-43.
- Nagayama S, Fukukawa C, Katagiri T, et al. Therapeutic potential of antibodies against FZD 10, a cell-surface protein, for synovial sarcomas. *Oncogene*. 2005;24:6201-6212.
- Fukukawa C, Hanaoka H, Nagayama S, et al. Radioimmunotherapy of human synovial sarcoma using a monoclonal antibody against FZD10. *Cancer Sci*. 2008;99:432-440.
- Giraudet A-L, Cassier PA, Iwao-Fukukawa C, et al. A first-in-human study investigating biodistribution, safety and recommended dose of a new radiolabeled MAb targeting FZD10 in metastatic synovial sarcoma patients. *BMC Cancer*. 2018;18:646.
- Kratochwil C, Bruchertseifer F, Giesel FL, et al. <sup>225</sup>Ac-PSMA-617 for PSMA-targeted alpha-radiation therapy of metastatic castration-resistant prostate cancer. *J Nucl Med*. 2016;57:1941-1944.
- Tafreshi NK, Doligalski ML, Tichacek CJ, et al. Development of targeted alpha particle therapy for solid tumors. *Molecules*. 2019;24(23):4314.
- Li HK, Sugyo A, Tsuji AB, et al. Alpha-particle therapy for synovial sarcoma in the mouse using an astatine-211-labeled antibody against frizzled homolog 10. *Cancer Sci*. 2018;109:2302-2309.
- Miederer M, Scheinberg DA, McDevitt MR. Realizing the potential of the Actinium-225 radionuclide generator in targeted alpha particle therapy applications. *Adv Drug Deliv Rev*. 2008;60:1371-1382.
- Sudo H, Tsuji AB, Sugyo A, et al. Preclinical evaluation of podoplanin-targeted alpha-radioimmunotherapy with the novel antibody NZ-16 for malignant mesothelioma. *Cells*. 2021;10:2503.
- Maguire WF, McDevitt MR, Smith-Jones PM, Scheinberg DA. Efficient 1-step radiolabeling of monoclonal antibodies to high specific activity with <sup>225</sup>Ac for alpha-particle radioimmunotherapy of cancer. *J Nucl Med*. 2014;55:1492-1498.
- Yoshida C, Tsuji AB, Sudo H, et al. Therapeutic efficacy of c-kit-targeted radioimmunotherapy using <sup>90</sup>Y-labeled anti-c-kit antibodies in a mouse model of small cell lung cancer. *PLoS One*. 2013;8:e59248.
- Eckerman KF, Endo A. *MIRD Radionuclide Data and Decay Schemes*, 2nd ed. Society of Nuclear Medicine; 2007; viii, 671 p.
- Behr TM, Sgouros G, Stabin MG, et al. Studies on the red marrow dosimetry in radioimmunotherapy: an experimental investigation of factors influencing the radiation-induced myelotoxicity in therapy with beta-, Auger/conversion electron-, or alpha-emitters. *Clin Cancer Res*. 1999;5:3031s-3043s.
- Sgouros G, Roeske JC, McDevitt MR, et al. MIRD pamphlet No. 22 (Abridged): radiobiology and dosimetry of  $\alpha$ -particle emitters for targeted radionuclide therapy. *J Nucl Med*. 2010;51(2):311-328.
- Sgouros G, Howell RW, Bolch WE, Fisher DR. MIRD commentary: proposed name for a dosimetry unit applicable to deterministic biological effects—the barendsen (Bd). *J Nucl Med*. 2009;50:485-487.
- Kawai A, Naito N, Yoshida A, et al. Establishment and characterization of a biphasic synovial sarcoma cell line, SYO-1. *Cancer Lett*. 2004;204:105-113.
- Larson SM, Carrasquillo JA, Cheung NK, Press OW. Radioimmunotherapy of human tumours. *Nat Rev Cancer*. 2015;15:347-360.
- Hanaoka H, Katagiri T, Fukukawa C, et al. Radioimmunotherapy of solid tumors targeting a cell-surface protein, FZD10: therapeutic efficacy largely depends on radiosensitivity. *Ann Nucl Med*. 2009;23:479-485.
- Nagayama S, Yamada E, Kohno Y, et al. Inverse correlation of the up-regulation of FZD10 expression and the activation of beta-catenin in synchronous colorectal tumors. *Cancer Sci*. 2009;100:405-412.
- Thurber GM, Schmidt MM, Wittrup KD. Antibody tumor penetration: transport opposed by systemic and antigen-mediated clearance. *Adv Drug Deliv Rev*. 2008;60:1421-1434.
- Ohshima Y, Sudo H, Watanabe S, et al. Antitumor effects of radionuclide treatment using alpha-emitting meta-<sup>211</sup>At-astato-benzylguanidine in a PC12 pheochromocytoma model. *Eur J Nucl Med Mol Imaging*. 2018;45:999-1010.
- Sudo H, Tsuji AB, Sugyo A, et al. Therapeutic efficacy evaluation of radioimmunotherapy with <sup>90</sup>Y-labeled anti-podoplanin antibody NZ-12 for mesothelioma. *Cancer Sci*. 2019;110:1653-1664.
- Song H, Hobbs RF, Vajravelu R, et al. Radioimmunotherapy of breast cancer metastases with alpha-particle emitter <sup>225</sup>Ac: comparing efficacy with <sup>213</sup>Bi and <sup>90</sup>Y. *Cancer Res*. 2009;69:8941-8948.
- Frost SHL, Frayo SL, Miller BW, et al. Comparative efficacy of <sup>177</sup>Lu and <sup>90</sup>Y for anti-CD20 pretargeted radioimmunotherapy in murine lymphoma xenograft models. *PLoS One*. 2015;10:e0120561.
- Khreish F, Ebert N, Ries M, et al. <sup>225</sup>Ac-PSMA-617/<sup>177</sup>Lu-PSMA-617 tandem therapy of metastatic castration-resistant prostate cancer: pilot experience. *Eur J Nucl Med Mol Imaging*. 2020;47:721-728.
- Zuo W, Zhao L. Recent advances and application of PD-1 blockade in sarcoma. *Onco Targets Ther*. 2019;12:6887-6896.
- Gorin J-B, Ménager J, Gouard S, et al. Antitumor immunity induced after  $\alpha$  irradiation. *Neoplasia*. 2014;16:319-328.
- Frampas E, Maurel C, Remaud-Le Saëc P, et al. Pretargeted radioimmunotherapy of colorectal cancer metastases: models and pharmacokinetics predict influence of the physical and radiochemical properties of the radionuclide. *Eur J Nucl Med Mol Imaging*. 2011;38:2153-2164.
- Behr TM, Sharkey RM, Juweid ME, et al. Phase I/II clinical radioimmunotherapy with an iodine-131-labeled anti-carcinoembryonic antigen murine monoclonal antibody IgG. *J Nucl Med*. 1997;38:858-870.
- O'Donoghue JA, Baidoo N, Deland D, Welt S, Divgi CR, Sgouros G. Hematologic toxicity in radioimmunotherapy: dose-response relationships for I-131 labeled antibody therapy. *Cancer Biother Radiopharm*. 2002;17:435-443.
- Emami B. Tolerance of normal tissue to therapeutic radiation. *Rep Radiother Oncol*. 2013;1:123-127.

36. Andrade-Campos MM, Liévano P, Espinosa-Lara N, et al. Long-term complication in follicular lymphoma: assessing the risk of secondary neoplasm in 242 patients treated or not with 90-yttrium-ibritumom ab-tiuxetan. *Eur J Haematol*. 2016;97:576-582.

#### SUPPORTING INFORMATION

Additional supporting information may be found in the online version of the article at the publisher's website.

**How to cite this article:** Sudo H, Tsuji AB, Sugyo A, et al. FZD10-targeted  $\alpha$ -radioimmunotherapy with  $^{225}\text{Ac}$ -labeled OTSA101 achieves complete remission in a synovial sarcoma model. *Cancer Sci*. 2022;113:721-732. doi:[10.1111/cas.15235](https://doi.org/10.1111/cas.15235)